**14th IEA Heat Pump Conference**
15-18 May 2023, Chicago, Illinois

# Experimental study of steam-driven ejector heat pump

Jeremy Spitzenberger [a], Ramy H. Mohammed [a], Pengtao Wang [a, b],
Hongbin Ma [a,*], Ahmad Abu-Heiba [c], Stephen Kowalski [b], Kashif Nawaz[b]

[a] Multiphysics Energy Research Center (MERC), College of Engineering, University of Missouri-Columbia, Columbia, MO 65211, USA.
[b] Multifunctional Equipment Integration Group, Building Technologies, Research and Integration Center (BTRIC), Oak Ridge National Laboratory, (ORNL), Oak Ridge, TN 37830.

**Abstract**

Ejector-driven systems have been shown to be promising for heating applications. Most of the research works have been devoted to cooling purposes, while little attention has been focused on heating applications. An experimental steam ejector heat pump system (EHP) was designed and constructed to assess its applicability to water heating applications. The effect of the primary nozzle exit position (NXP) on the performance of the steam ejector system was investigated for a primary nozzle throat diameters of 1.5 mm and 2.0 mm. The ejector system was run for high-temperature evaporator (HTE) temperatures of 120, 130, and 140 ˚C and low-temperature evaporator (LTE) temperatures of 10, 15 and 20 ˚C. The target of this investigation was to attain the highest condensing temperature to be able to use the proposed system for water heating purposes. The ejector heat pump coefficient of performance (EHP COP) was used to determine the system efficiency. Larger LTE temperatures were found to result in higher EHP COPs and condensing temperatures. A maximum EHP COP of 2.02 was attained for a HTE and LTE temperatures 120 ˚C and 20 ˚C, respectively, however only resulted in a condensing temperature of 22.88 ˚C. Higher HTE temperatures were found to result in higher condensing temperatures, but at the cost of EHP COP.



*Keywords: Type your keywords here, separated by semicolons ;*

## 1. Introduction

In the United States an estimated 18% of residential energy consumption is use ford domestic hot water (DHW) production [1], however a significant portion of the energy required to power these systems is lost in the delivery process, coming in the form of waste heat. Studies have found the more electrically driven a DHW heater is, the higher the primary energy loss will be in the generation and transmission process, and by increasing the share of DHW heaters powered by natural gas, the primary energy efficiency of the system can increase by as much as 65% [2]. These findings indicate an opportunity to pursue the idea of utilizing thermally driven heat pumps for DHW production. Not only are they able to eliminate the primary energy losses in the transmission process of electrical energy, but also, they are able to integrate the waste heat by recycling it back into the system, therefore, they can deliver more useful energy than they consume. A 2015 study conducted by the Lawrence Livermore National Laboratory estimated waste heat accounted for 60% of the total US energy consumption, with 75% of that waste heat being at a temperature of 230 °C or less [3]. If this excess thermal energy can be recycled back into a heat pump system, the electricity demand of a heat pump can be decreased by as much as 80% [4].

Presently, the thermally driven heat pump sector is dominated by sorption technologies [5]. However, research in this sector is ongoing and still at a relatively low maturity level. More research is needed to develop a deeper and more fundamental understanding of the working mechanisms and system performances. One field that has shown promise and great market potential are thermally driven ejector heat pump (EHP) systems. Research on thermally driven ejector systems have been conducted in the past for refrigeration purposes, these are known as ejector refrigeration systems (ERSs). Ejector driven systems are seen as an attractive option as they require little maintenance due to their lack of moving parts and do not require high ozone potential refrigerant to operate, thus helping to reduce our carbon footprint. Despite this, research on ERS systems has found that these systems yield lower COPs compared to the vapor compression refrigeration systems which continue to dominate the market [6]. Recently there has been a resurgence in ERS research due to a growing environmental concern, yet EHP systems remain relatively untouched. This lack of interest could be attributed to the historical difficulty in understanding the theoretical efficiency of the ejector cycle [7].

A typical ejector system consists of a HTE, LTE, ejector, pump, throttling valve, and a condenser, as seen in Figure 1a. The primary fluid (PF) is superheated in the HTE, which is then accelerated through a converging-diverging nozzle, reaching supersonic speeds at the nozzle exit position (NXP). This creates a low-pressure which leads to a suction effect of the secondary fluid (SF) within the LTE, thus, entraining water vapor into the suction chamber, which leads to a cooling effect. The two steams mix in the mixing chamber and then experience a normal shock at some point along the constant area section. This leads to a sharp increase in pressure and decrease in the velocity of the fluid flow. The fluid mixture then continues to decelerate as it travels along the diffuser and is eventually ejected into the condenser where the fluids then enter a reservoir and are returned to the LTE and HTE through a throttling valve and pump, respectively. The pressure and velocity profiles are shown in Figure 1b.

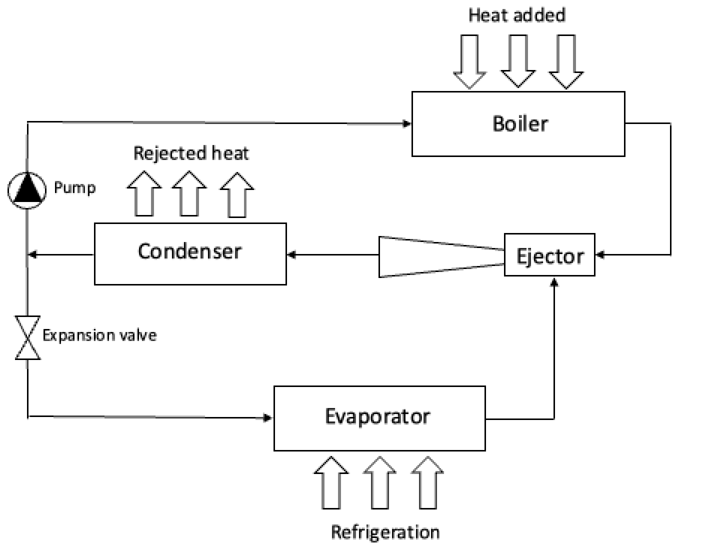


(a)

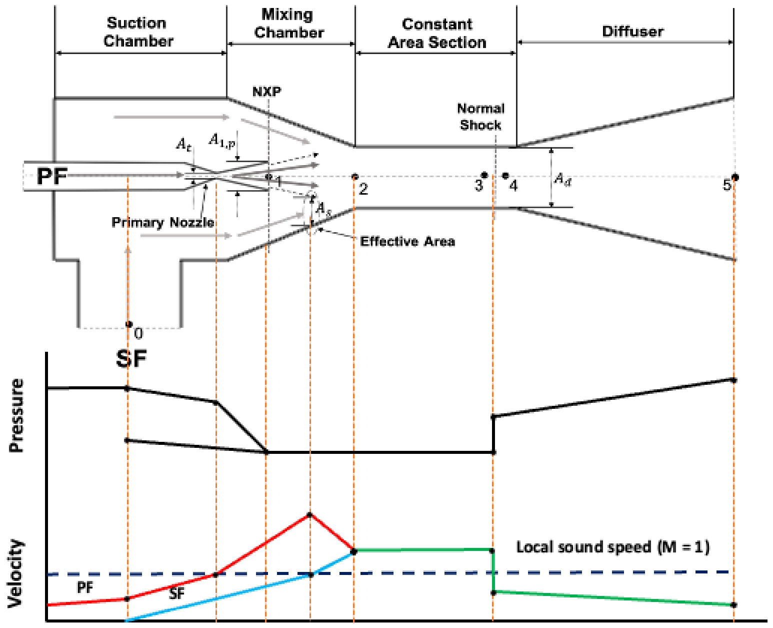


(b)

Figure 1: (a) Schematic of typical ejector cycle and (b) pressure and velocity profiles of fluid flow along ejector.

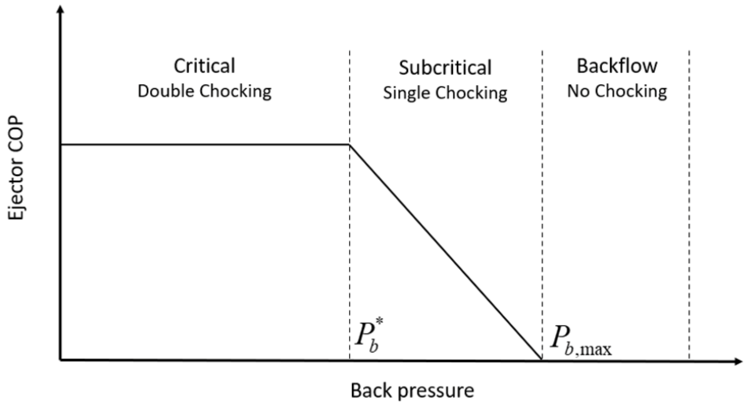


Figure 2: Effect of back pressure on the COP of an ejector

Most ejector experimental studies found in literature focus on operating the ejector system under critical conditions, meaning both the primary and secondary fluids being chocked at their inlets, due to the fact it will result in the highest COPs, as shown in Figure 2. Despite this, the theoretical results from Spitzenberger et al [8], suggest that for an EHP system a high $COP_{EJT}$ does not necessarily correlate to a high COP for the EHP, rather the ejector should be operated within the subcritical zone, in order to maximize the $P_b$, to achieve the highest condensing temperature possible. The goal of this investigation is focused on the ejector cycle to try and achieve the maximum condensing temperature possible, in order to develop the single-stage gas-fired ejector heat pump water heater first proposed in Spitzenberger et al [8] , which aims to produce a domestic hot water (DHW) supply 14.5 ℃ to a target delivery temperature of 51.7 ℃.

## 2. Experimental

In this section, the experimental setup in addition to the function of each component is discussed in detail. Error propagation in the COP of the EHP is determined based on the uncertainty of each variable.

### *2.1. Experimental setup description*

A schematic and image of the experimental setup is shown in Figure 3. The power inputs into the HTE and LTE were supplied by two electrical resistance immersion heaters, connected to a variable voltage transformer capable of supplying 240 V to the system. These allowed the heat added to the HTE and LTE to be set to a specific value to be able to control the pressure and temperature of the working fluid within each vessel. The condenser was a shell-in-tube heat exchanger, consisting of a stainless-steel shell and copper tubing, designed to have a cooling capacity of 7 kW. The cooling fluid was supplied by a constant temperature thermal bath (Maxi Cool Recirculating chiller-RC150-C0021) set to deliver water at a temperature of 14.5 °C to simulate domestic tap water [7].

The input voltages across the electrical heaters within the HTE and LTE were monitored using the Keithley 2701 digital multimeter which had an accuracy of 4% [9]. Type-T thermocouples with an accuracy of ± 0.5 ℃ were used to measure the temperature of the PF in the HTE, SF in the LTE, condenser, and the inlet and outlet temperatures of the cooling water across the condenser. Pressure transducers with an accuracy of 0.08% were installed in the HTE, LTE and condenser to monitor their internal pressures. In addition to this, pressure taps were added along the ejector's axis to measure the static pressure profile along the ejector.

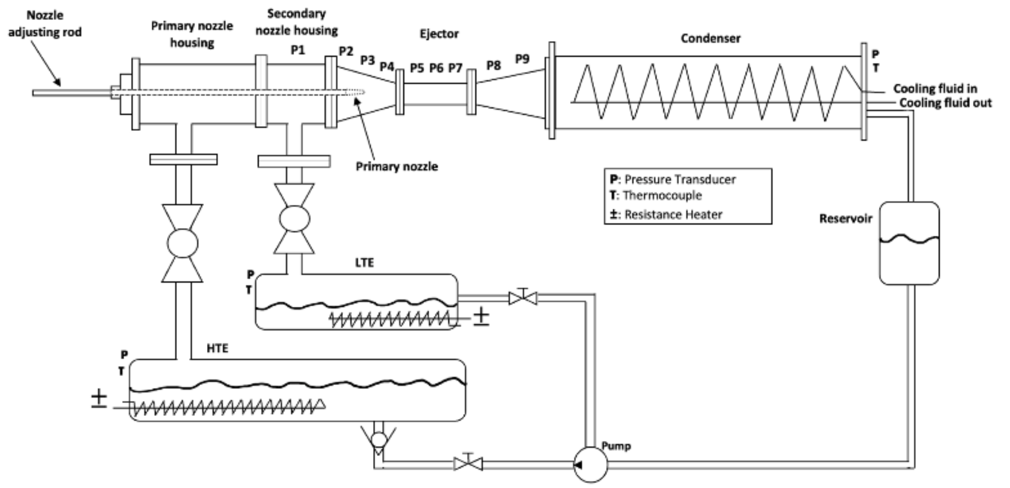


**(a)**

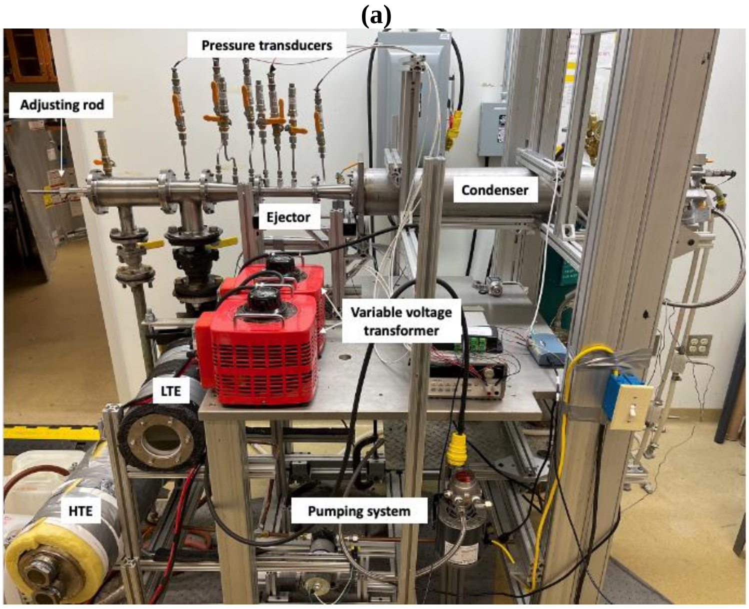


**(b)**

Figure 3: (a) Schematic and (b) picture of EHP experimental setup

The heating capacities within the HTE, LTE, along with the cooling capacity in the condenser are calculated using:

$$\dot{Q}_{LTE} = I \times V \quad \text{and} \quad \dot{Q}_{HTE} = I \times V \tag{1}$$

$$\dot{Q}_c = \dot{m}_w c_p (T_{out} - T_{in}) \tag{2}$$

where $I$ is the current, $V$ is the voltage, $\dot{m}_w$ is the cooling water mass flow rate, and $T_{out}$ and $T_{in}$ are the cooling water outlet and inlet temperatures, respectively.

Energy losses within the system were estimated by performing an energy balance across the entire system. Comparing the sum of the thermal load from the HTE and LTE to the condenser cooling capacity. The difference between the two was always found to be less than 4% indicating the system was well insulated. The pumping power was assumed to be negligible compared to the input power into the HTE, therefor the heating-cycle COP of the EHP is determined from [7]:

$$COP_{EHP} = \frac{\dot{Q}_c}{\dot{Q}_{HTE}} \tag{3}$$

Tests were run of HTE temperatures of 120 – 140 °C and LTE temperatures of 10 – 20 °C for primary nozzles with throat diameters of 1.5 and 2 mm. Additional trials were run at LTE temperatures of 25 and 30 °C for the 1.5 mm primary nozzle throat.

### *2.2. Uncertainty Analysis*

To ensure the reliability of the experimental measurements, a few of the trials were repeated three times under the same operating conditions, and the COP values were calculated and compared. The deviation between the similar tests were found to be less than 3%, thus indicating the repeatability and reliability of the experimental setup and measurements. The relative error is estimated by

$$\left(\delta_{COP_{EHP}}\right)^2 = \left(\frac{\partial COP_{HP}}{\partial \dot{Q}_c}\delta_{\dot{Q}_c}\right)^2 + \left(\frac{\partial COP_{HP}}{\partial \dot{Q}_{HTE}}\delta_{\dot{Q}_{HTE}}\right)^2 \tag{4}$$

where

$$\left(\delta_{\dot{Q}_c}\right)^2 = \left(\frac{\partial \dot{Q}_c}{\partial \Delta T_w}\delta_{\Delta T_w}\right)^2 + \left(\frac{\partial \dot{Q}_c}{\partial \dot{m}_w}\delta_{\dot{m}_w}\right)^2 \tag{5}$$

$$\left(\delta_{\dot{Q}_{HTE}}\right)^2 = \left(\frac{\partial \dot{Q}_{HTE}}{\partial I}\delta_I\right)^2 + \left(\frac{\partial \dot{Q}_{HTE}}{\partial V}\delta_V\right)^2 \tag{6}$$

and it is found that it is about 6.5%.

## 3. Results and Discussion

The pressure profiles inside the ejector are presented at various LTE and HTE temperatures to attempt to understand they affect the flow behaviour withing the ejector and ultimately the performance of the EHP COP. This section ends with a performance diagram that summarizes the COP and back pressure at various operating conditions.

### *3.1. Effect of HTE temperature*

The temperature of the HTE can be changed by adjusting the input voltage to the heater. The pressure profile along the ejector at various HTE temperatures can be observed in Figure 4. It can be observed that when the HTE temperature was increased from 120 °C to 140 °C, the backpressure rose from 2.8 to 3.4 kPa, corresponding to temperatures of 22.88 °C and 26.12 °C, respectively. It should be noted that the first three pressure transducers from the left to right, read the pressures of the entrained flow from the LTE to be nearly the same. Starting at the P4, the variations in the pressure reading were observed, thus indicating the pressure during the mixing process is not constant. The pressure was then observed to increase then decrease at P5, which is in the constant area section. A pressure drop is then observed at P6 and P7, which is a result of an increase in the velocity of the fluid flow. The normal shock appeared to take place somewhere between P7 and P8, which lead to a sharp increase in the static pressure and decrease in the flow velocity. Beyond that, the pressure continued to increase, as the steam travelled along the divergent diffuser section.

The pressure variation depends on the HTE temperature, which controls the mixing pressure and pressure rise across the normal shock. From Figure 4, it can be observed that an increase in HTE temperature from 120 °C to 130 °C, resulted in a 0.29 kPa increase in the backpressure (P9). When the HTE temperature was further increased to 140 °C, the backpressure reached 3.36 kPa, with is 0.53 kPa higher than a HTE temperature of 120 °C. Based on these results it can be concluded that an increase in the HTE can help to attain larger backpressures and in turn larger condensing temperature, thus increasing the temperature life of the heat pump, however, this also results in lower EHP COPs, as shown in Figure 5. The EHP COP was found to decrease from 2.02 to 1.62, when the HTE temperature dropped from 140 °C to 120 °C, which is ~20% decrease in the EHP COP.

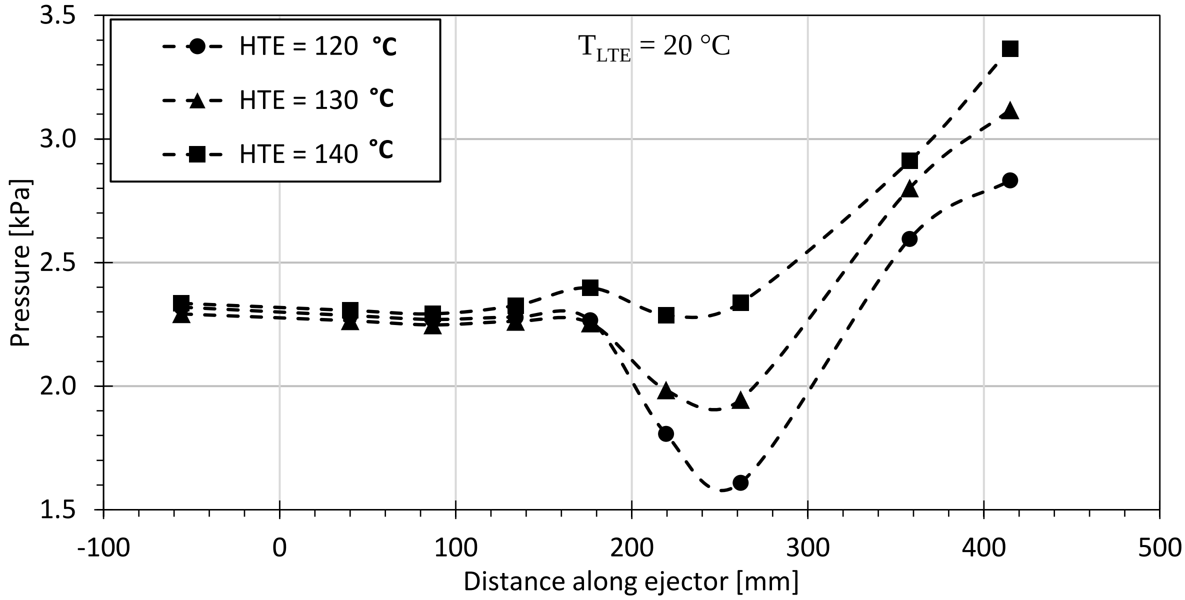


Figure 4: Pressure profile along the ejector at various HTE temperatures for nozzle throat diameter of 1.5 mm.

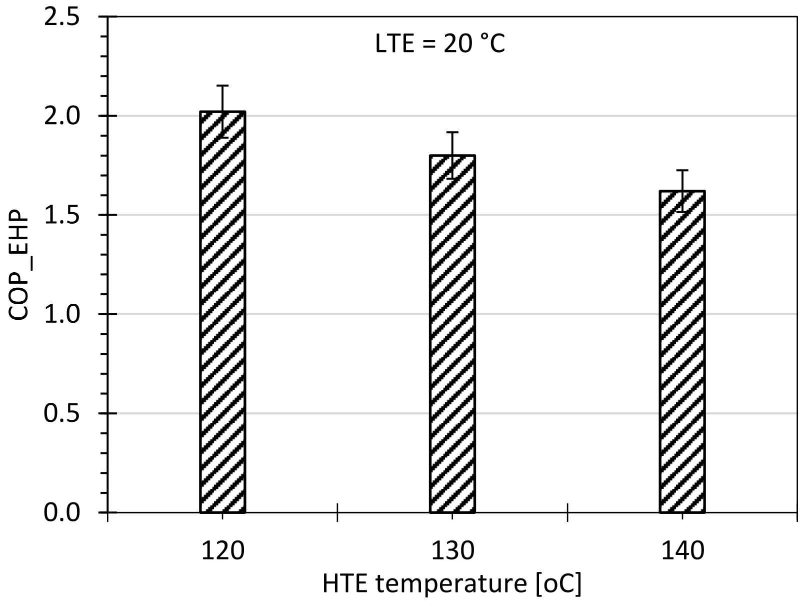


Figure 5: HTE temperature effect on the EHP COP using a nozzle throat diameter of 1.5 mm

### *3.2. Effect of LTE temperature*

The pressure profile along the ejector at various LTE temperatures can be seen in Figure 6. It can be observed that the pressure rises when the LTE temperature increases. For each of the trials the pressures decreased slightly as the steam travelled along the first three pressure transducers, then at the fourth pressure transducer, the pressure was found to significantly depend on the LTE temperature. As shown in Figure 6, a LTE temperature of 20 °C resulted in the largest backpressure. At lower LTE temperatures, a lower amount of water vapor is entrained into the mixing chamber, and the vapor that is entrained has less momentum.

As shown in Figure 7, the temperature of the LTE has a significant effect on the EHP COP, which was found to increase as the LTE temperature increased. A 140% improvement in the EHP COP was observed when the LTE temperature was increased from 10 °C to 20 °C, 1.28 and 1.80, respectively. More importantly, not only did increasing the LTE temperature increase the EHP COP, it also resulted in increased backpressures or temperature life of the heat pump.

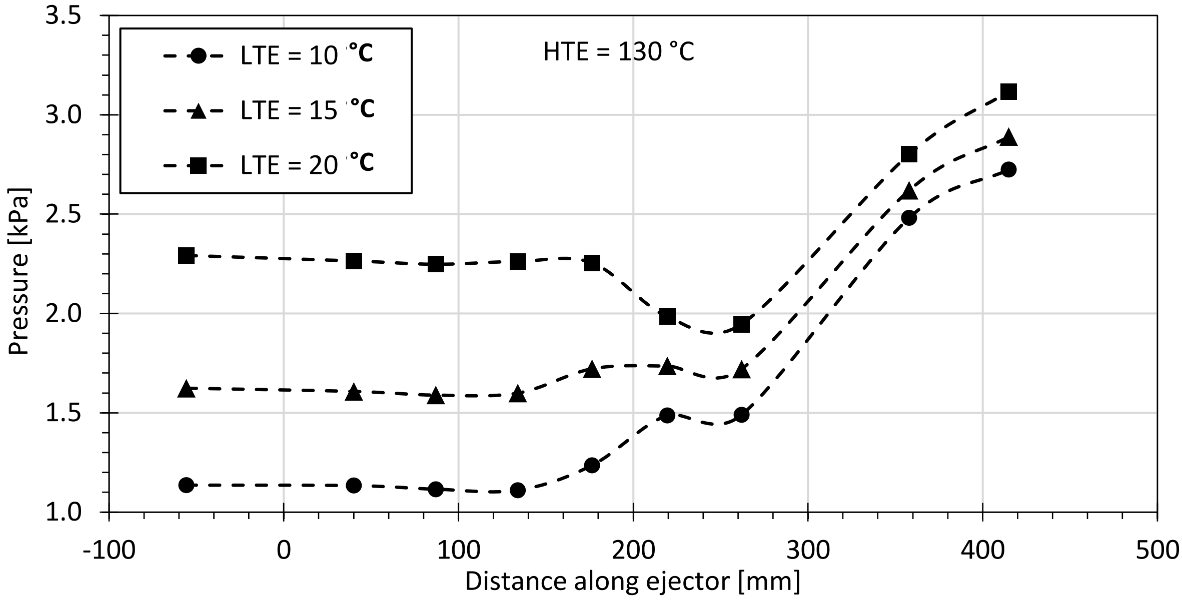


Figure 6: Pressure profile along the ejector at various LTE temperatures for nozzle throat diameter of 1.5 mm.

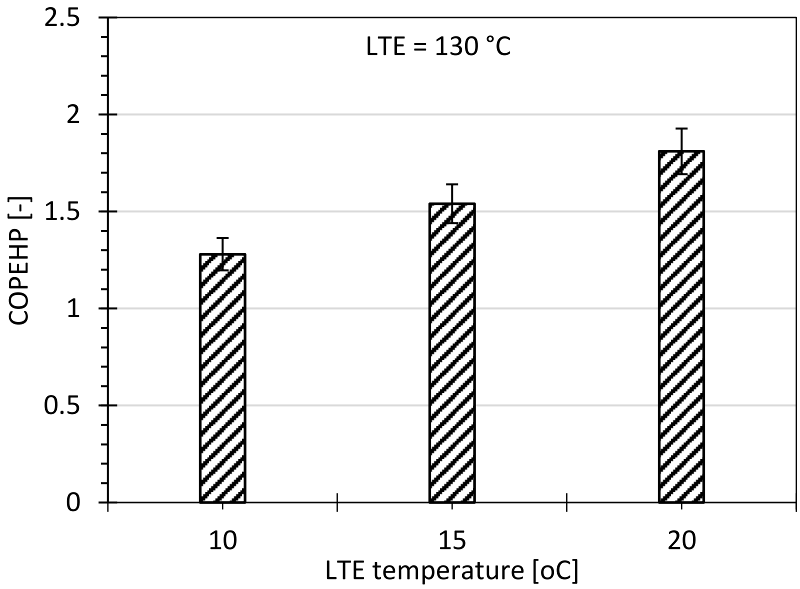


Figure 7: Effect of LTE temperature on the COP of EHP using a nozzle throat diameter of 1.5 mm.

### *3.3. Effect of nozzle throat diameter*

The EHP COP for the two different primary nozzles can be observed in Figure 8. It was found that the nozzle with the smaller throat diameter, 1.5 mm, performed better than that with the 2.0 mm throat diameter. A decrease in the throat diameter, resulted in a decrease in the mass flow rate of the PF travelling through the nozzle. This is also directly related to the heat input to the HTE, which in turn results in a significant increase in the EHP COP. At a nozzle exit position of 0.40, the EHP COP improved from 1.40 to 1.80, a 29% improvement, when the nozzle throat sized was decreased from 2.0 mm to 1.5 mm. A larger backpressure was able to be attained with the 2.0 mm nozzle. This trend shows that a smaller throat size is preferred for larger EHP COPs, while a larger throat diameter is better for larger backpressures. This result emphasizes the importance of optimizing the primary nozzle geometry to find the best compromise between EHP COP and backpressure.

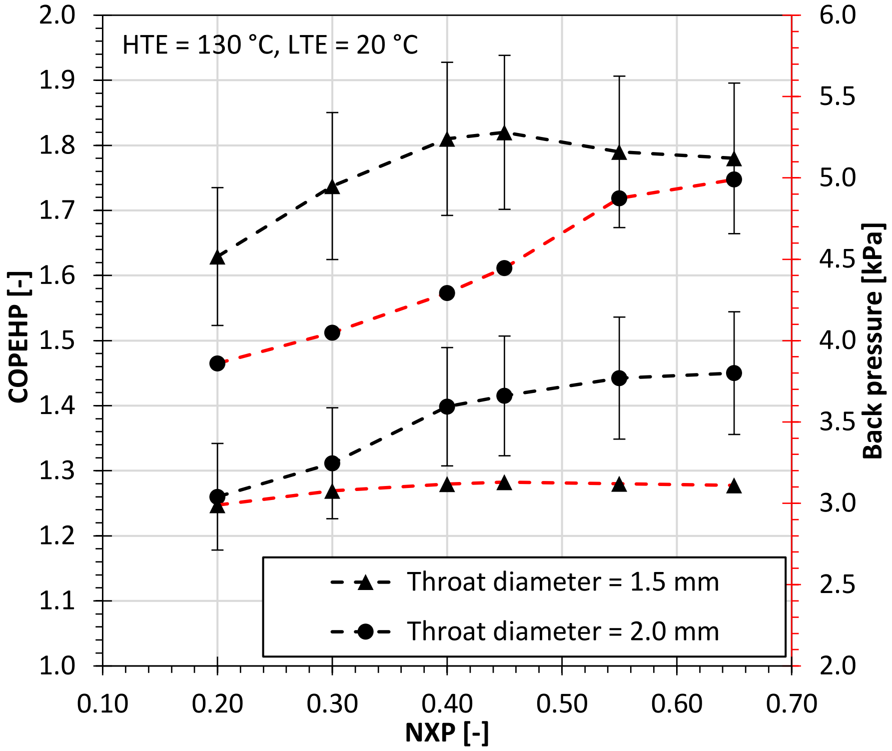


Figure 8: EHP COP and back pressure using two different throat diameters at various NXPs

### *3.4. Ejector performance*

A performance diagram depicting the EHP COP and backpressure at various operating conditions for the 1.5 mm nozzle can be seen in Figure 9. Larger LTE temperatures were found to correspond to larger EHP COPs and backpressures, while larger HTE temperatures resulted in lower EHP COPs and larger backpressures. It is found that to increase the backpressure or temperature lift of an EHP, the EHP COP will need to be sacrificed. The EHP map shown in Figure 9 can be used to select the idea working conditions that provide a compromise between the EHP COP and backpressure, that will best suit the requirements of the EHP system. It should be noted at the values will change with the nozzle size however, the general trend will remain the same.

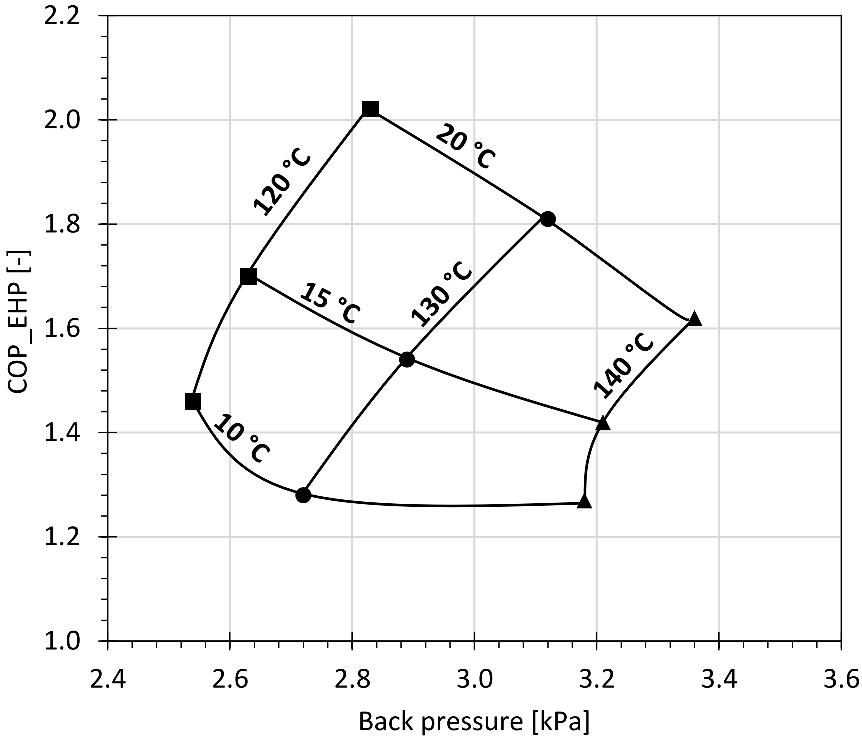


Figure 9: Performance map of EHP using a 1.5 mm nozzle at NXP of 0.40.

## 4. Conclusion

In this work, on a steam-driven ejector heat pump for water heating purposes was built and tested to determine the effects of the operating conditions and design parameters of the EHP COP and backpressure under sub-critical conditions. Nine pressure transducers were installed along the axis of the ejector to observe the effects the operating conditions had on the static pressure profile of the steam as it travels through the ejector. The experimental results indicate larger LTE temperatures are better for larger EHP COPs and backpressures or a larger temperature lift for the EHP, while larger HTE temperatures also lead to higher backpressures, but the EHP COP is compromised. A larger throat diameter resulted in lower EHP COPs and larger backpressures. Therefore, it is important to carefully design a primary nozzle to get the desired trade-off between the EHP COP and backpressure. An ejector performance map is provided to help select the operating conditions for the desired set point for the EHP system. From this investigation it can be concluded that further work needs to be done to further develop a clear understanding of the behaviour of the fluid flow through an ejector, which can then be used to further improve the EHP system.

**Acknowledgements**

This material is based upon work supported by the U.S. Department of Energy, Office of Science, Building Technologies Office. This research used resources of the Building Technologies Research and Integration Center (BTRIC) of the Oak Ridge National Laboratory, which is a DOE Office of Science User Facility.

**References**

[1] Fuentes, E., Arce, L., and Salom, J. "A Review of Domestic Hot Water Consumption Profiles for Application in Systems and Buildings Energy Performance Analysis." *Renewable and Sustainable Energy Reviews*, Vol. 81, No. February 2017, 2018, pp. 1530–1547. https://doi.org/10.1016/j.rser.2017.05.229.

[2] Abu-Heiba Oak Ridge, TN (United States)] (ORCID:0000000153356180), A. [Oak R. N. Lab. (ORNL). "Literature Review of Potential Thermally Activated Heat Pump Cycles." 2018.

[3] Forman, C., Muritala, I. K., Pardemann, R., and Meyer, B. "Estimating the Global Waste Heat Potential." *Renewable and Sustainable Energy Reviews*, Vol. 57, 2016, pp. 1568–1579. https://doi.org/10.1016/j.rser.2015.12.192.

[4] Ayyoub, M. M., Abu-heiba, A., and Vineyard, E. *Multi-Function Gas Fired Heat Pump*. Oak Ridge, TN (United States), 2015.

[5] Dias, J. M. S., and Costa, V. A. F. "Adsorption Heat Pumps for Heating Applications: A Review of

Current State, Literature Gaps and Development Challenges." *Renewable and Sustainable Energy Reviews*, Vol. 98, No. August, 2018, pp. 317–327. https://doi.org/10.1016/j.rser.2018.09.026.

[6] Pounds, D. A., Dong, J. M., Cheng, P., and Ma, H. B. "Experimental Investigation and Theoretical Analysis of an Ejector Refrigeration System." *International Journal of Thermal Sciences*, Vol. 67, 2013, pp. 200–209. https://doi.org/10.1016/j.ijthermalsci.2012.11.001.

[7] Wang, P., Ma, H., Spitzenberger, J., Abu-Heiba, A., and Nawaz, K. "Thermal Performance of an Absorption-Assisted Two-Stage Ejector Air-to-Water Heat Pump." *Energy Conversion and Management*, Vol. 230, 2021. https://doi.org/10.1016/j.enconman.2020.113761.

[8] Spitzenberger, J., Wang, P., Ismael, L., Ma, H., Abuheiba, A., and Nawaz, K. "Theoretical Analysis of a Single-Stage Gas-Fired Ejector Heat Pump Water Heater." *Journal of Thermal Science and Engineering Applications*, Vol. 14, No. 4, 2022, pp. 1–10. https://doi.org/10.1115/1.4051708.

[9] Keithley 2010 Series: 7.5 Digit Multimeter with Scanning | Tektronix n.d. https://www.tek.com/en/products/keithley/digital-multimeter. Accessed Nov. 9, 2022.